PHYSICAL REVIEW A **88**, 043841 (2013)

Quantum interferometric lithography with pair-coherent states

Yan-Xiao Gong*

Department of Physics, Southeast University, Nanjing 211189, People's Republic of China

(Received 16 August 2013; published 28 October 2013)

We investigate a quantum interferometric lithography system using pair-coherent states as resources to excite an N-photon recording medium. The interference pattern is found to have half the period of the classical light interference pattern limited by the Rayleigh criterion. The fringe visibility is nearly unity in the low-flux region and decreases with increasing values of the average photon number. We show that as N increases, the high-flux limit visibility increases and the bright-fringe width decreases; however, the fringe period and spacing remain the same. Compared with the results using two-mode squeezed vacuum states, although our results have the same high-flux limit visibility, we can get higher contrast and narrower bright-fringe patterns under the same conditions of light flux and lithography material. Our approach sheds light on quantum lithography with nonclassical light and reveals how pair-coherent states can be superior to two-mode squeezed vacuum states.

DOI: 10.1103/PhysRevA.88.043841 PACS number(s): 42.50.St, 42.50.Dv, 42.50.Ex

I. INTRODUCTION

Photonic quantum technologies have aroused great interest in the past decades [1]. One of the practical applications is known as quantum lithography, first proposed by Boto *et al.* in 2000 [2], which is to exploit entangled states of light to beat the Rayleigh criterion in interferometric optical lithography. The Rayleigh criterion states that the resolution of a traditional optical lithography system is limited by diffraction and the minimum resolvable feature size is half the wavelength of the illuminating light. Explicitly, they showed theoretically that by using N-photon path-entangled states, that is, the NOON states of the form $(|N,0\rangle + |0,N\rangle)/\sqrt{2}$, interference patterns with a resolution N times greater than the Rayleigh resolution limit could be written on the N-photon absorbing material. It has been shown that in principle any pattern can be written using a variety of entangled states of light [3,4].

In spite of several proof-of-principle experimental demonstrations of quantum lithography [5,6], many challenges still exist for a real practical application. One of the major difficulties is the requirement of a bright entangled light source that is strong enough to excite the multiphoton recording medium. In experiments, the two-photon NOON state required for two-photon lithography can be easily produced through a Hong-Ou-Mandel (HOM) interferometer [7] with photon pairs from a spontaneous parametric down-conversion source. However, this method can only work in the low-flux region, while in the high-flux region, where this source is often called an unseeded optical parametric amplifier (OPA), the HOM interference visibility and thus the lithography pattern contrast decrease due to the multiphoton contamination [8–10]. More explicitly, the entangled state of light generated from an unseeded OPA is the two-mode squeezed vacuum state (TMSVS) given by

$$|\Psi_s\rangle = \operatorname{sech} g \sum_{n=0}^{\infty} (e^{i\varphi}\tanh g)^n |n,n\rangle, \tag{1}$$

where g represents the single-pass gain and φ is a phase parameter. It was shown that the lithography pattern visibility decreases from unity to an asymptotic value of 20% as g increases from 0 to ∞ and such a feature has been observed in experiment [11]. Then this result was generalized to the case of N-photon absorbing material [12]. It was revealed that as N increases, the high-gain limit visibility increases, but the pattern period and spacing remain the same with the case of $N = 2$. A recent approach [13] utilizing an optical parametric oscillator obtained coinciding results with those using an OPA.

In this paper, we consider a possible method to suppress the multiphoton contamination and improve the lithography pattern by modifying the joint photon number distribution for the superposition of twin-Fock states of the form $\sum_{n=0}^{\infty} C(n)|n,n\rangle$. For this aim, here we investigate the use of a kind of twin-Fock superposition state, the pair-coherent state (PCS), which can be written in the following form in Fock state bases [14]:

$$|\Psi_p\rangle = \mathcal{N} \sum_{n=0}^{\infty} \frac{\xi^n}{n!} |n,n\rangle, \tag{2}$$

where ξ is a complex number and $\mathcal{N} = 1/\sqrt{I_0(2|\xi|)}$ is the normalization factor with $I_0(2|\xi|)$ denoting the modified Bessel function of the first kind of order zero. Similar to the usual single-mode coherent states which are the eigenstates of the annihilation operator, the PCSs are the eigenstates of the product of twin-beam annihilation operators, $\hat{a}_1\hat{a}_2|\Psi_p\rangle = \xi|\Psi_p\rangle$, with the restriction $(\hat{a}_1^\dagger\hat{a}_1 - \hat{a}_2^\dagger\hat{a}_2)|\Psi_p\rangle = 0$. It has been shown that the PCSs could be produced by competition between four-wave mixing and amplified spontaneous emission in resonant two-photon excitations [14], by a nondegenerate parametric oscillator [15,16], by a two-mode photon matching process using weak cross-Kerr media [17], or by projective measurement on a pair of ordinary coherent states [18]. The PCSs have aroused much interest since in contrast to the TMSVSs, they are non-Gaussian states and have several properties such as sub-Poissonian statistics and violations of Bell inequalities [19–22]. Applications of PCSs in continuous-variable quantum-information processing have been explored [23–25]. In particular, a very recent approach [26] showed that the PCSs are superior to the TMSVSs in parity-measurement-based optical phase measurements and both Heisenberg-limited phase uncertainty and super-resolution can be realized with the PCSs.

*gongyanxiao@gmail.com

In this paper, we reveal another advantage of PCSs against TMSVSs in the field of quantum lithography. We show that the lithography patterns for PCSs and TMSVSs have similar features including the same period, spacing, and high-flux limit visibility when exciting an N-photon recoding medium, but the PCS pattern has a higher visibility and a narrower bright-fringe width than the TMSVS under the same average photon number. The rest of the paper is organized as follows. In the next section we study the features of PCSs for use in two-photon quantum lithography. In Sec. III we investigate the lithography features when an arbitrary N-photon recording medium is used, with comparisons with the features of TMSVSs. Conclusions and discussions are given in Sec. IV.

II. QUANTUM LITHOGRAPHY WITH A TWO-PHOTON RECORDING MEDIUM

Figure 1 shows a typical quantum interferometric optical lithography setup [2]. An entangled light produced from the generator first interferences at a balanced beam splitter (BS) and then the output two arms of light excite a photon recording medium, inducing a lithography pattern which depends on the path length difference, or equivalently the relative phase shift ϕ. The field at the photon recording medium can be expressed as

$$\hat{a}_5 = (e^{i\phi}\hat{a}_3 + \hat{a}_4)/\sqrt{2}. \tag{3}$$

We write the operator transformations at the BS in the form

$$\hat{a}_3 = (\hat{a}_1 + \hat{a}_2)/\sqrt{2}, \quad \hat{a}_4 = (\hat{a}_1 - \hat{a}_2)/\sqrt{2}. \tag{4}$$

Combining Eqs. (3) and (4) we get

$$\hat{a}_5 = [(1 + e^{i\phi})\hat{a}_1 - (1 - e^{i\phi})\hat{a}_2]/2. \tag{5}$$

The photon recording rate at the an N-photon absorbing lithography medium is proportional to the N-photon absorbing rate

$$P^{(N)} = \langle \Psi_i | \hat{a}_5^{\dagger N} \hat{a}_5^N | \Psi_i \rangle. \tag{6}$$

We first calculate the case of $N = 2$. In the beginning, we first consider the twin-Fock state $|M\rangle_1|M\rangle_2$ as an initial state. From Eqs. (5) and (6) we can straightforwardly obtain the two-photon absorbing rate as

$$\begin{aligned} P_{MM}^{(2)} &= \langle M,M|\hat{a}_5^{\dagger 2}\hat{a}_5^2|M,M\rangle \\ &= \frac{M}{4}[5M - 3 - (M+1)\cos 2\phi]. \end{aligned} \tag{7}$$

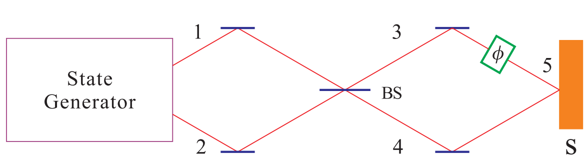

FIG. 1. (Color online) Schematic of quantum interferometric optical lithography by exciting a photon recording medium (S) with quantum entangled states of light. BS represents the balanced beam splitter. Numbers label the beams.

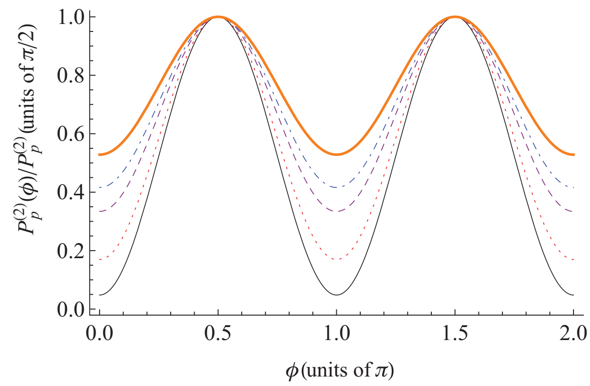

FIG. 2. (Color online) Two-photon absorbing rates $P_p^{(2)}(\phi)$ of the PCS as functions of ϕ (in units of π) for average photon numbers $\bar{N}_p = 0.1$ (thin solid line), 0.4 (dotted line), 1 (dashed line), 1.5 (dot-dashed line), 3 (thick solid line).

Then with the PCS given by Eq. (2) as the initial state, we can write the two-photon absorbing rate as

$$\begin{aligned} P_p^{(2)} &= \mathcal{N}^2 \sum_{n=0}^{\infty} \frac{|\xi|^{2n}}{(n!)^2} \langle n,n|\hat{a}_5^{\dagger 2}\hat{a}_5^2|n,n\rangle \\ &= \frac{1}{4}(5|\xi|^2 - 3\bar{N}_p)\left[1 - \frac{|\xi|^2 + \bar{N}_p}{5|\xi|^2 - 3\bar{N}_p}\cos(2\phi)\right], \end{aligned} \tag{8}$$

where $\bar{N}_p$ denotes the average photon number in each mode of the initial state, which can be given by

$$\bar{N}_p = \langle \Psi_p|\hat{a}_1^\dagger \hat{a}_1|\Psi_p\rangle = \mathcal{N}^2 \sum_{n=0}^{\infty} \frac{|\xi|^{2n}}{(n!)^2} n = \frac{|\xi| I_1(2|\xi|)}{I_0(2|\xi|)}. \tag{9}$$

Equation (8) shows that the two-photon absorbing rate as a function of the phase shift ϕ has a period of π which is half of the classical period of 2π. The fringe behaviors for different average photon numbers $\bar{N}_p$ are plotted in Fig. 2. We can see that as $\bar{N}_p$ increases, the fringe visibility decreases and explicitly the visibilities are 91%, 71%, 50%, 41%, 31% for $\bar{N}_p = 0.1$, 0.4, 1, 1.5, 3, respectively. Here the fringe visibility is defined as $V \equiv (P_{\max} - P_{\min})/(P_{\max} + P_{\min})$. Analytically, Eq. (8) gives the fringe visibility as $V_p^{(2)} = (|\xi|^2 + \bar{N}_p)/(5|\xi|^2 - 3\bar{N}_p)$, which approaches 20% in high-flux limit, i.e., when $|\xi| \to \infty$. The behaviors of $V_p^{(2)}$ against $\bar{N}_p$ are plotted in Fig. 3. Despite being much lower than unity, the visibility in the high-flux region is believed to be large enough for many practical applications [8–10,12,13].

We now compare our results with the lithography fringe using the TMSVS to excite a two-photon absorbing medium. Such results have been given in Refs. [8–10,12]; however, here equivalently, we revisit the features via calculations in the Fock state bases. Considering the TMSVS given by Eq. (1) as the initial state and combining Eq. (7), we can write the two-photon absorbing rate for the TMSVS as

$$\begin{aligned} P_s^{(2)} &= \operatorname{sech}^2 g \sum_{n=0}^{\infty} \tanh^{2n} g \langle n,n|\hat{a}_5^{\dagger 2}\hat{a}_5^2|n,n\rangle \\ &= \frac{1}{2}\bar{N}_s(5\bar{N}_s + 1)\left[1 - \frac{1 + \bar{N}_s}{1 + 5\bar{N}_s}\cos(2\phi)\right], \end{aligned} \tag{10}$$

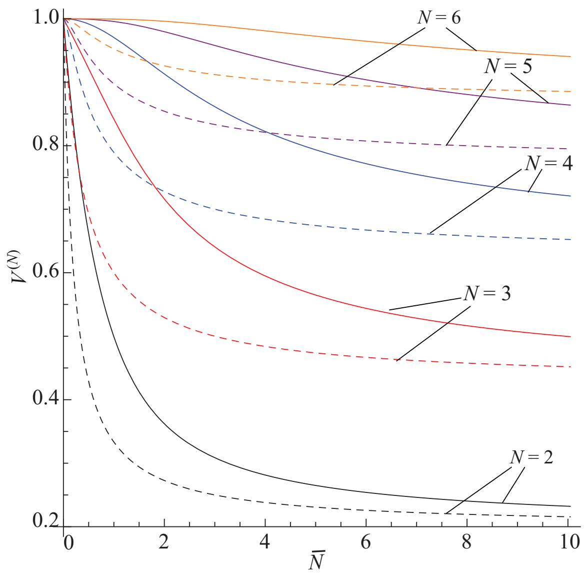

FIG. 3. (Color online) N-photon absorbing fringe visibilities $V^{(N)}$ vs average photon numbers $\bar{N}$ for the PCS (solid line) and TMSVS (dashed line).

where the average photon number in one mode is

$$\bar{N}_s = \langle \Psi_s | \hat{a}_1^\dagger \hat{a}_1 | \Psi_s \rangle = \sinh^2 g. \quad (11)$$

From Eqs. (8) and (10) we can see clearly that the two-photon absorbing rates for PCS and TMSVS have similar relations with the phase shift ϕ and different visibility expressions. The fringe visibility for the TMSVS is $V_s^{(2)} = (1 + \bar{N}_s)/(1 + 5\bar{N}_s)$, which approaches 20% when $\bar{N}_s \to \infty$. The behaviors of $V_s^{(2)}$ against $\bar{N}_s$ are also shown in Fig. 3. We can see that despite the same high-flux limit visibility, the fringe contrast for the PCS decreases slower than that for the TMSVS with increasing $\bar{N}$. That means that under the condition of the same average photon number, the PCS can write a higher contrast fringe than the TMSVS on the two-photon recording medium.

III. QUANTUM LITHOGRAPHY WITH MULTIPHOTON RECORDING MEDIUM

We now investigate the interferometric lithography behaviors using the PCS to excite an arbitrary N-photon recording medium. With Eqs. (5) and (6), we can calculate the N-photon absorbing rate for a twin-Fock state $|M,M\rangle (2M \geqslant N)$ as

$$P_{MM}^{(N)} = \frac{N!}{2^N} \sum_{k=\min\{0,N-M\}}^{\max\{N,M\}} \binom{N}{k} \binom{M}{k} \binom{M}{N-k} \times (1+\cos\phi)^{N-k}(1-\cos\phi)^k. \quad (12)$$

Then the N-photon absorbing rate for the PCS is

$$P_p^{(N)} = \mathcal{N}^2 \sum_{n=0}^{\infty} \frac{|\xi|^{2n}}{(n!)^2} P_{nn}^{(N)}. \quad (13)$$

The analytic expressions for an arbitrary N-photon absorbing rate can be calculated by the above two equations. For instance, the three- and four-photon absorbing rates are given by

$$P_p^{(3)} = \tfrac{1}{2}\{(1+5r^2)\bar{N}_p - r^2 - 3[r^2 - (1-r^2)\bar{N}_p]\cos^2\phi\}, \quad (14)$$

$$P_p^{(4)} = \tfrac{1}{8}\{r^2(6+35r^2) - 2(3+10r^2)\bar{N}_p - 6[r^2(5r^2-6) + 2(3+2r^2)\bar{N}_p]\cos^2\phi + 3[r^2(2+r^2) + 2(2r^2-1)\bar{N}_p]\cos^4\phi\}. \quad (15)$$

The behaviors of N-photon absorbing rates against the phase shift ϕ for $N = 2, 3, 4, 5, 6$ with average photon numbers $\bar{N}_p = 0.4$ and $\bar{N}_p = 3$ are plotted in Figs. 4(a) and 4(b). We can see that with increasing N, the fringe visibility increases and the bright fringe becomes narrower, but the fringe period and spacing remain the same. In particular, we may obtain the fringe visibilities $V_p^{(N)}$ through Eqs. (12) and (13), which are plotted in Fig. 3 for $N = 2, 3, 4, 5, 6$ as functions of average photon numbers $\bar{N}_p$. It reveals again an improved visibility with a high-order multiphoton recording medium and, explicitly, the analytic high-flux limit visibilities for $N = 3, 4, 5, 6$ can be found to be 3/7, 27/43, 55/71, 215/247, respectively. In the high-flux limit, a visibility of 99% can be obtained with a 10-photon recoding medium. We can also get the full width at half maximum of the bright fringe, the behaviors of which versus the average photon

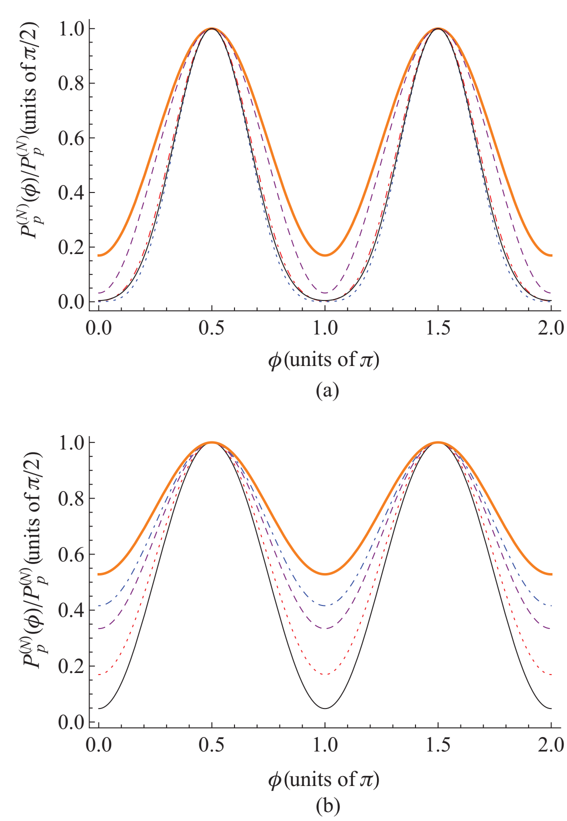

FIG. 4. (Color online) N-photon absorbing rates $P_p^{(N)}(\phi)$ of the PCS as functions of ϕ (in units of π) for $N = 2$ (thick solid line), 3 (dashed line), 4 (dot-dashed line), 5 (dotted line), and 6 (thin solid line), with an average photon number (a) $\bar{N}_p = 0.4$ and (b) $\bar{N}_p = 3$.

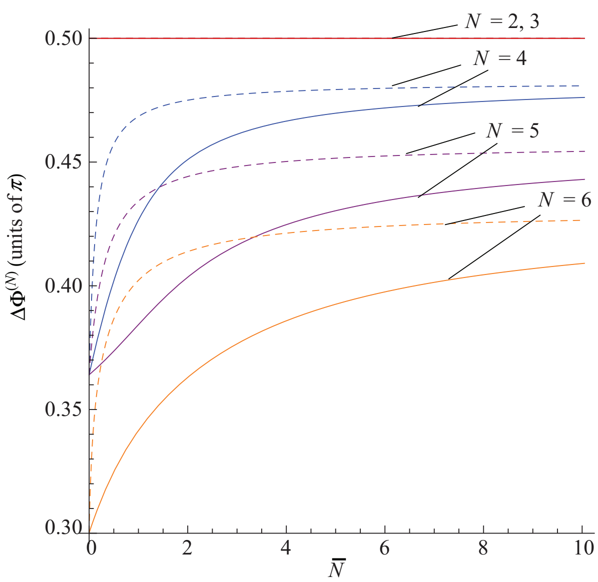

FIG. 5. (Color online) FWHM $\Delta\Phi$ (in units of π) of N-photon absorbing fringe for the PCS (solid line) and the TMSVS (dashed line) vs average photon number $\bar{N}$.

numbers for $N = 2, 3, 4, 5, 6$ are shown in Fig. 5. We should note that the FWHM is obtained by $\Delta\Phi^{(N)} = \pi - 2\phi_0$, where ϕ_0 is the solution in $\{0,\pi/2\}$ to the equation $P_p^{(2)}(\phi) = [P_p^{(2)}(0) + P_p^{(2)}(\pi/2)]/2$. We can see that as N increases the FWHM of the bright fringe decreases.

The results for the TMSVS exciting an arbitrary N-photon recording medium have been given in Refs. [12,13]. Here, equivalently, we can calculate the N-photon absorbing rate for the TMSVS by

$$P_s^{(N)} = \text{sech}^2 g \sum_{n=0}^{\infty} \tanh^{2n} g \, P_{nn}^{(N)}. \qquad (16)$$

The behaviors of the fringe visibility and bright-fringe FWHM are also plotted in Figs. 3 and 5, respectively. We may find that the lithography fringes of the PCS and TMSVS have similar features including the same period, spacing, and high-flux limit visibility; however, with the same average photon number, the PCS fringe has a higher visibility and a narrower bright-fringe width under the same order multiphoton absorbing medium.

To this end, we would like to give some remarks on why the PCS displays advantages over the TMSVS. From Eq. (12) we can find that as $M(2M \geqslant N)$ increases, the N-photon absorbing fringe visibility for the twin-Fock state $|M,M\rangle$ decreases from unity to the high-flux limit given in the above calculations. As shown in Ref. [26], the joint photon number distribution for the TMSVS is thermal-like and peaked for the vacuum state. However, the joint photon number distribution for the PCS is highly peaked for the twin-Fock state $|m,m\rangle$ with $m \sim \bar{N}$. Consequently, under the same average photon number the PCS has a higher visibility than TMSVS. Analogous reasoning leads to the narrower bright fringe for the PCS than for the TMSVS.

IV. CONCLUSIONS AND DISCUSSIONS

In summary, we have theoretically investigated a quantum interferometric lithography system employing PCSs to excite an N-photon recoding medium. We have found that the phase-shift period of the lithography fringe is half of the period allowed by the Rayleigh criterion. This feature exists even in the high-flux region, with only a decreased visibility. We have shown that as the photon absorbing order N increases, the visibility may increase and the FWHM of the bright fringe may decrease, but the fringe period and spacing remain the same. We have made comparisons between the lithography features of the PCS and the TMSVS. We found that they have the same fringe period, spacing, and high-flux limit visibility; but under the same average photon number and photon-absorbing order, the PCS fringe has a higher visibility and a narrower bright-fringe FWHM.

We should note that despite only a twofold enhancement over the standard Rayleigh limit, the method developed here is still meaningful to the field of lithography due to the advantages of quantum lithography over conventional interferometric lithography [27] in terms of cost, efficiency, and quality. Moreover, the interferometric techniques exploiting nonclassical states could be used in combination with the techniques developed in sub-Rayleigh lithography based on classical methods [28,29].

We would like to briefly discuss the experimental challenges of our scheme. One of them is the realization of multiphoton recording materials. Actually, finding new lithographic materials is crucial to both quantum lithography schemes and some classical lithography models. In addition, multiphoton absorbing materials have broad applications in many other fields, for instance, in optical imaging [30]. Great efforts have been made to develop such materials (for an introductory review, see Ref. [31]). It should be mentioned that there has been much discussion on whether certain properties of entangled light may make N-photon absorption more, or less, likely than with classical light, independent of the properties of the absorbing medium. Tsang [32,33] argued that N-photon absorption is less likely, while in contrast, Plick*et al.* [34] argued that it is more likely.

Another challenge lies in the experimental production of the PCS. Unlike the experimentally feasible TMSVS source, a PCS has not been produced in experiment to date. As we stated, due to good nonclassical features the PCS has proved to be more suitable for parity-measurement-based high-precision phase measurement than the TMSVS [26]. We hope our approach can stimulate more investigations on the production and application of PCS. Finally, our approach opens a door to quantum interferometric lithography. We hope our work can stimulate more development on new light sources and new lithographic materials for quantum lithography.

ACKNOWLEDGMENTS

This work was supported by the State Key Program for Basic Research of China (Grant No. 2011CBA00205) and the National Natural Science Foundations of China (Grant No. 11004096).

[1] J. L.O'Brien, A. Furusawa, and J. Vučković, Nat. Photon. **3**, 687 (2009).
[2] A. N. Boto, P. Kok, D. S. Abrams, S. L. Braunstein, C. P. Williams, and J. P. Dowling, Phys. Rev. Lett. **85**, 2733 (2000).
[3] P. Kok, A. N. Boto, D. S. Abrams, C. P. Williams, S. L. Braunstein, and J. P. Dowling, Phys. Rev. A **63**, 063407 (2001).
[4] G. Björk, L. L. Sánchez-Soto, and J. Söderholm, Phys. Rev. Lett. **86**, 4516 (2001).
[5] M. D'Angelo, M. V. Chekhova, and Y. Shih, Phys. Rev. Lett. **87**, 013602 (2001).
[6] S. Rosen, I. Afek, Y. Israel, O. Ambar, and Y. Silberberg, Phys. Rev. Lett. **109**, 103602 (2012).
[7] C. K. Hong, Z. Y. Ou, and L. Mandel, Phys. Rev. Lett. **59**, 2044 (1987).
[8] G. S. Agarwal, R. W. Boyd, E. M. Nagasako, and S. J. Bentley, Phys. Rev. Lett. **86**, 1389 (2001).
[9] E. M. Nagasako, S. J. Bentley, R. W. Boyd, and G. S. Agarwal, Phys. Rev. A **64**, 043802 (2001).
[10] E. M. Nagasako, S. J. Bentley, R. W. Boyd, and G. S. Agarwal, J. Mod. Opt. **49**, 529 (2002).
[11] F. Sciarrino, C. Vitelli, F. De Martini, R. Glasser, H. Cable, and J. P. Dowling, Phys. Rev. A **77**, 012324 (2008).
[12] G. S. Agarwal, K. W. Chan, R. W. Boyd, H. Cable, and J. P. Dowling, J. Opt. Soc. Am. B **24**, 270 (2007).
[13] H. Cable, R. Vyas, S. Singh, and J. P. Dowling, New J. Phys. **11**, 113055 (2009).
[14] G. S. Agarwal, Phys. Rev. Lett. **57**, 827 (1986).
[15] M. D. Reid and L. Krippner, Phys. Rev. A **47**, 552 (1993).
[16] A. Gilchrist and W. J. Munro, J. Opt. B: Quantum Semiclassical Opt. **2**, 47 (2000).
[17] Y.-L. Dong, X.-B. Zou, and G.-C. Guo, Phys. Lett. A **372**, 5677 (2008).
[18] C. C. Gerry, J. Mimih, and R. Birrittella, Phys. Rev. A **84**, 023810 (2011).
[19] G. S. Agarwal, J. Opt. Soc. Am. B **5**, 1940 (1988).
[20] K. Tara and G. S. Agarwal, Phys. Rev. A **50**, 2870 (1994).
[21] A. Gilchrist, P. Deuar, and M. D. Reid, Phys. Rev. Lett. **80**, 3169 (1998).
[22] A. Gilchrist, P. Deuar, and M. D. Reid, Phys. Rev. A **60**, 4259 (1999).
[23] V. C. Usenko and B. I. Lev, Phys. Lett. A **348**, 17 (2005).
[24] A. Gábris and G. S. Agarwal, Int. J. Quant. Inform. **05**, 17 (2007).
[25] V. C. Usenko and M. G. Paris, Phys. Lett. A **374**, 1342 (2010).
[26] C. C. Gerry and J. Mimih, Phys. Rev. A **82**, 013831 (2010).
[27] C. Williams, P. Kok, H. Lee, and J. P. Dowling, Inform. Forsch. Entw. **21**, 73 (2006).
[28] S. J. Bentley and R. W. Boyd, Opt. Express **12**, 5735 (2004).
[29] H. J. Chang, H. Shin, M. N. O'Sullivan-Hale, and R. W. Boyd, J. Mod. Opt. **53**, 2271 (2006).
[30] W. R. Zipfel, R. M. Williams, and W. W. Webb, Nat. Biotechnol. **21**, 1369 (2003).
[31] R. W. Boyd and J. P. Dowling, Quant. Inf. Process. **11**, 891 (2012).
[32] M. Tsang, Phys. Rev. A **75**, 043813 (2007).
[33] M. Tsang, Phys. Rev. Lett. **101**, 033602 (2008).
[34] W. N. Plick, C. F. Wildfeuer, P. M. Anisimov, and J. P. Dowling, Phys. Rev. A **80**, 063825 (2009).